Particle distribution mechanisms in infusion molded composites

S.P. Fernberg[1], T.S. Lundström[2], E.J. Sandlund[1], I.Öhgren[1]

[1] SICOMP AB, P.O. Box 271, SE-941 26 Piteå, Sweden
[2] Luleå University of Technology, Division of Fluid Mechanics, SE-971 87 Luleå, Sweden

ABSTRACT

The present paper presents results from an experimental investigation on infusion molding where two grades of commercially available ATH-filler (with different particle size distributions) are added to the liquid resin. In the study we have performed infusion experiments which subsequently were analyzed using conventional mould filling flow modeling and microscopy studies. Viscosities of the suspensions were also measured to further facilitate the analysis. Based on the results, potential key mechanisms controlling resin flow and hence also the final particle distribution are proposed and discussed. A pore-doublet model was proposed to explain the observation that regions with high particle concentrations were found everywhere in the particle filled laminates. The observation that these highly concentrated regions are located where shear strain rates are expected to be low suggests that they are generated as a consequence of a Bingham-type of viscosity behavior observed for the suspension.

1. INTRODUCTION

Development of composite materials manufactured by infusion molding is of increasing interest partially because the method offers high quality materials at comparably low cost. This has been recognized by many manufacturers and end-users e.g. within the transportation sector.

The accelerating usage of particles such as aluminatrihydroxide (ATH) in resin infusion manufacturing techniques has mainly been motivated by the difficulties of fulfilling requirement on fire resistance with conventional composites [1]. To maximize the effect of the particles it is of importance to understand and control the mechanisms that governs the dispersion of the particles within a laminate during processing. The present study is therefore focused on identifying key mechanisms that govern final particle distribution within a laminate that is manufactured by resin infusion techniques. Although initially driven by the particular need for understanding the manufacturing process of fire resistant composite materials, our ambition is that the outcome should be knowledge of generic nature that ultimately will facilitate controlled manufacturing with any particles that fulfill certain assumptions. Examples of other filler materials that may be of interest are nano-sized particles e.g. nano-clays, hollow glass spheres or microcapsules containing healing agents to be used in self healing composites [2].

During recent years a substantial amount of research has been devoted to develop understanding and models for infusion with conventional thermoset matrix systems [3-6]. Infusion with particle filled systems however implies additional complexity.

2. THEORY

Darcy's law is, for a one-dimensional flow given by

$$\frac{Q}{A} = \frac{K}{\mu}\frac{\Delta p}{L} \tag{1}$$

where Q denotes the volumetric flow rate, A is the cross sectional area of the porous channel, μ is the viscosity of the fluid and Δp represents the pressure drop measured over a flow distance L. The constant K is the constitutive property of the porous media termed

permeability. By applying the integral form of Eq. (1) the flow front position x at time t can be expressed as:

$$x^2 = \frac{2K}{\mu}\frac{\Delta p}{(1-V_f)}t \tag{2}$$

where V_f denotes the volume fraction of fiber. Hence, the shear viscosity of a particle filled resin suspension is of major importance for the macroscopic flow during infusion. A number of models for suspension viscosities have been proposed in the literature e.g. by Ball and Richmond (1980); Krieger and Dougherty (1959) [7] and by Patton (1964) [8]. All of these models rely on empirical calibrations of experimentally determined viscosities. An evaluation of several models [9] showed that the model proposed by Krieger and Dougherty had the best correlation to experimental data. This model states that the suspension viscosity η can, be found from the following equation:

$$\eta = \eta_s\left(1-\phi/\phi_m\right)^{-[\eta]\phi_m} \tag{3}$$

where η_s is the viscosity of the suspending medium (i.e. the neat resin), ϕ is the phase volume of filler (i.e. the volume fraction of particles in the suspending medium), ϕ_m is the maximum packing fraction of particles and $[\eta]$ denotes the number which in suspension rheology terms is called intrinsic viscosity.

3. MATERIALS

The resin system used throughout this study was CRYSTIC U 904 LVK, an orthoptalic resin designed for vacuum infusion. The resin was cured by the aid of 1.1% methyl ethyl ketone peroxide (Norpol No 1) and 0.2% NLC 10 inhibitor. Two grades of ATH-particles, MARTINAL OL 104 and MARTINAL ON 310, were used as fillers in the suspensions. The main difference between the two grades is the particle size distribution. Characteristic particle sizes of OL 104 vary between 0.5 and 5 μm i.e. 90 % of the particles are found within that range. The median particle size of OL 104 filler is 2 μm. The corresponding range for ON 310 is 2 - 25 μm with the median at 8 μm. The reinforcement used in the experiments was a Vetrotex RT 800 from Saint-Gobain Technical Fabrics. This is a plain glass fiber weave with an average surface weight of 816 g/m^2. The fabric is made from 2400 tex glass fiber yarns in both warp and weft direction.

4. EXPERIMENTAL

Viscosity measurements were performed using a CVO Rheometer and a matching analyzing software from Bohlin Instruments Ltd. Empirical shear stress vs. shear strain rate curve, at a temperature of 25 °C, were obtained for each suspension by varying the straining rate. Shear strains rates were typically varied between 0.1 and 500 s^{-1} in the measurements. The indicated viscosities were determined using values obtained for shear strains rates in the range between 1 and 20 s^{-1}. Five particle concentrations corresponding to filler weight fractions W_f of 0.05, 0.10, 0.20 0.30 and 0.50 were tested for suspensions B to D, see Table 1.

Table 1. Constituents of ATH-filled suspensions and sample geometry used during viscosity measurements.

Suspension designation	Base resin	Filler	Rheometer sample geometry
Susp A	CRYSTIC U 904 LVK	-	Plate and cup
Susp B	CRYSTIC U 904 LVK	OL 104	Cone and plate
Susp C	CRYSTIC U 904 LVK	ON 310	Cone and plate
Susp D	CRYSTIC U 904 LVK	2/3 of OL 104 + 1/3 of ON 310	Cone and plate

The suspensions A-D were also used in vacuum infusion experiments. In this case the filler volume fraction, ϕ, of suspensions B-D was kept constant at $\phi = 0.395$. Each experiment involved simultaneous infusion of four different preforms, see Fig. 1. Each preform consisted of a stack containing five layers of the Vetrotex fabric. The width w was 300 mm for all preforms. Preform length y_{tot} varied in the dimensions y_{tot} = 50, 100, 150 and 200 mm. Stacks were, during the experiments placed according to Fig. 1 on a flat metal table and covered with a flexible bag. A plastic spiral was used as distribution channel. The spiral was positioned along one side of the reinforcement so that infusion from one edge and thus the desired one-dimensional parallel flow would be attained. Tacky-tape was used to seal the bag onto the table to create the closed cavity containing the preforms which is required for vacuum infusion composite manufacturing. The polyester suspension was degassed for five minutes prior to infusion. The flow fronts in each preform were continuously monitored throughout the manufacturing and the position and shape of the flow front were marked on the bag at regular time intervals. The outlets of the individual preforms, connected to the vacuum pump through a single pipe, were individually closed once the actual preform was completely filled, see Fig. 1. A manometer positioned at the outlet registered the level of vacuum supplied by the vacuum pump.

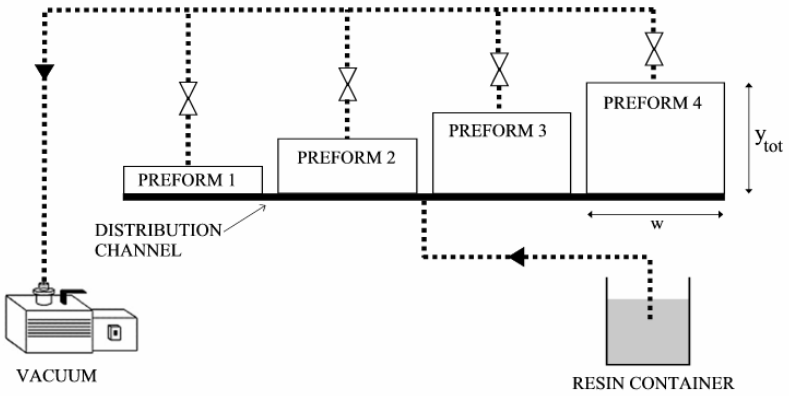

Fig. 1. Schematic drawing of experimental setup used during vacuum infusion experiments.

Microscopy analysis on the final microstructure of the laminates was performed on polished cross-sections taken from selected locations of the laminates and cast in resin. Polishing was performed in a Struers Pedemat, Rotopol polishing machine using silicon carbide paper applied in successive steps from 180 to 4000 grit, and in a final step, Buehler Mastermet polishing suspension. An Olympus BHSM-F optical microscope equipped with a Color View 1 digital camera was used to study and acquire digital images. Software provided by Soft Imaging Systems GmbH, AnalySIS Docu, was used for the subsequent image analysis. Fiber volume fraction, V_f, of the laminates were determined by the burn-off technique.

5. RESULTS AND DISCUSSION

The viscosity of the neat resin was measured to be 151 mPas which is slightly higher than the values from the manufacturer, η = 100 - 140 mPas. It is still lower than for all other suspensions, see Table 2. The viscosity is generally increasing with decreasing particle size at a constant filler volume fraction. Some deviations from this principle is observed at low particle concentrations, see Table 2. The small discrepancies presented above may be attributed to the fact that the viscosity of each concentration and suspension was only measured once.

From the results it was not possible to state any clear tendency of onset of shear thinning behavior at higher strain rates. A few samples exhibited a slight tendency for shear thinning at strain rates above approximately 100 s^{-1} whereas the other exhibited linear stress vs. strain rate response over the entire test range. No definite conclusions regarding e.g. onset of shear thinning tendency could thus be drawn. Estimations of the maximum strain rates during our experiments however elucidate the necessity of taking any possible non-linear shear thinning effects into consideration, the suspensions can be considered as Newtonian.

Table 2. Results from viscosity measurements.

Suspension	W_f	ϕ	η [Pas]	σ_y [Pa]
Susp A	0	0	0.151	-
Susp B	0.05	0.103	0.194	-
	0.10	0.195	0.271	-
	0.20	0.353	0.325	-
	0.30	0.483	0.632	-
	0.50	0.686	19.00*	10.3*
Susp C	0.05	0.103	0.176	-
	0.10	0.195	0.260	-
	0.20	0.353	0.236	-
	0.30	0.483	0.353	-
	0.50	0.686	2.25	-
Susp D	0.05	0.103	0.168	-
	0.10	0.195	0.216	-
	0.20	0.353	0.262	-
	0.30	0.483	0.393*	4.6*
	0.50	0.686	3.99*	5.2*

* values obtained by assuming a so-called Bingham behavior

High concentration suspensions of Susp B and Susp D exhibited a Bingham type of behavior in the experiments. This implies that no viscous flow occurs until a certain shear stress (the yield stress σ_y) is exceeded. This observation is in agreement with previous work in which it was found that a Bingham type of behavior is often observed for suspensions [10-12], particularly at high particle concentrations. The yield stress σ_y indicated in Table 2 are obtained by extrapolation to zero shear strain rate of a straight line fit of experimental data.

We can see from Fig. 2 that the proposed model (Eq. (3)) is capable of reproducing the experimental results in Table 2. The parameters, ϕ_m and $[\eta]$, required for calibration of the model were obtained by using Matlab 6.1 ver. 12.1 together with a pre-defined optimization function *Fminsearch*. This routine enables numerical minimization of the discrepancy between experimental results and the model. The minimized quantity was

$$\sigma^2 = \sum_{i=1}^{i=n} \left(f(\phi_m, [\eta], \phi_i) - \eta_{\phi_i} \right)^2 \quad (4)$$

where $f(\phi_m, [\eta], \phi_i)$ denotes the predicted viscosity by the proposed model (Eq. 3) obtained for a certain particle volume fraction ϕ_i, η_{ϕ_i} is the measured viscosity at the corresponding ϕ_i. Output from the minimization is the parameters ϕ_m and $[\eta]$ that yield in the smallest value of σ^2 i.e. the best fit of experimental results to the model. The following parameters were obtained for our experimental results: Susp B: ϕ_m = 0.697, $[\eta]$ = 1.687; Susp C: ϕ_m = 0.695, $[\eta]$ = 0.890 and Susp D: ϕ_m = 0.697, $[\eta]$ = 1.139.

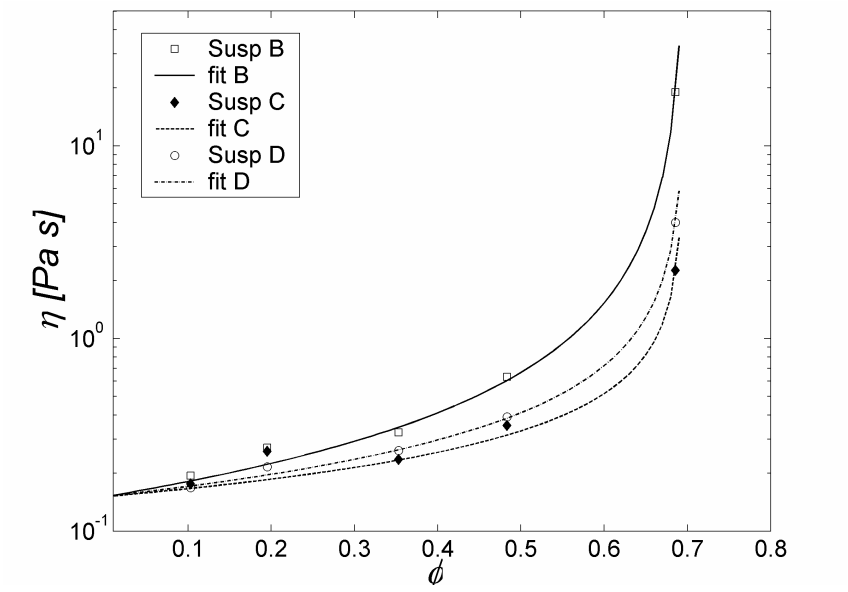

Fig. 2. Experimentally determined shear viscosities vs. filler volume fraction ϕ of the different ATH-fillers. Lines indicate optimal fit of viscosity model given by Eq. (3).

A general feature of the infusion experiments was that unexpectedly high irregularities of the flow fronts were observed. The irregularity was particularly high for infusions with particle filled suspensions. The irregularities are partially due to the comparably coarse meso-scale structure of the plain weave (see e.g. Fig. 3) which apparently makes five fabric layers insufficient to generate a reinforcement stack with a homogeneous permeability. The observation that irregularities were particularly pronounced for particle filled suspensions gives support to the hypothesis that the presence of particles influences the flow associated with infusion. The registered times required to completely fill the molds followed the expected behavior i.e. shortest mold filling time was observed for suspensions with low viscosities. Mold filling times for the 200 mm long preform (rightmost in Fig. 1) were approximately 6 minutes for Susp A; 10 minutes for Susp C; 14 minutes for Susp D and 16 minutes for Susp B.

Microscopy samples taken close to the inlet and near the outlet were carefully studied in order to detect differences in particle concentrations, see e.g. Fig. 3-5. This did not, however, reveal any obvious discrepancies. It was instead found that all cross-sections had areas with extremely high particle concentration, see Fig. 3 and 4. The areas appear in the cavities between the bundles of the plain weave glass fiber reinforcement where a majority of the resin

flow takes place during infusion i.e. in the flow channels They are always formed or connected to locations where this flow channel seems to have a particularly small or narrow dimension e.g. at the intersection of two fiber bundle surfaces. Furthermore it is observed that the particle areas always have contact with a fiber bundle.

The micrographs in Fig. 5 show the fiber bundles at higher magnification. Interestingly the ATH-particles are also located within the bundles, preferably in resin rich areas. Qualitative estimations based on our microscopy studies indicate: i) the amount of particles present in the bundles is higher for suspensions with small particles compared to suspensions with larger particles, ii) the matrix particle concentration is lower within a bundle as compared to within a flow channel. Conclusions are based on observations that particles are generally not dispersed within all cavities between individual fibers in a bundle. This is particularly obvious in laminates with larger particles where large parts of the bundles are impregnated by neat resin only.

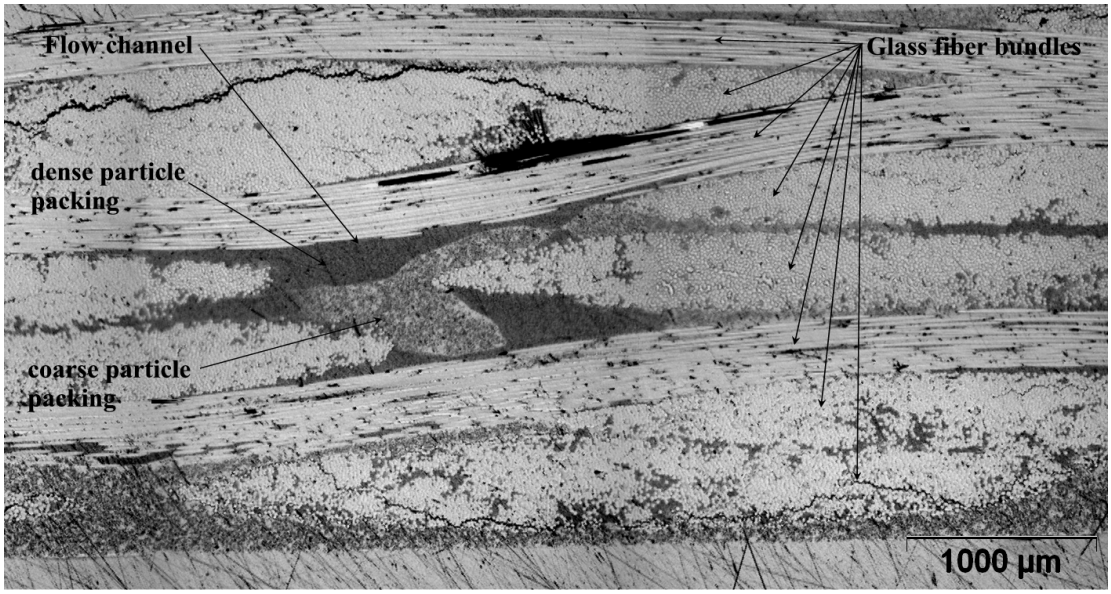

Fig. 3. Micrograph of polished cross-section of laminates with Susp B matrix.

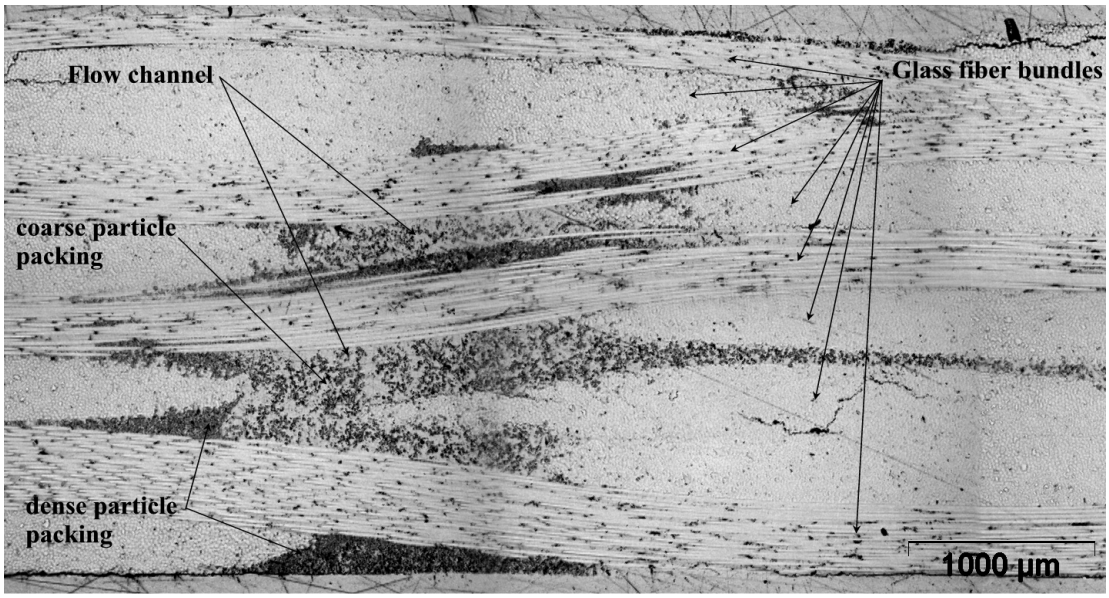

Fig. 4. Micrograph of polished cross-section of laminates with Susp C matrix

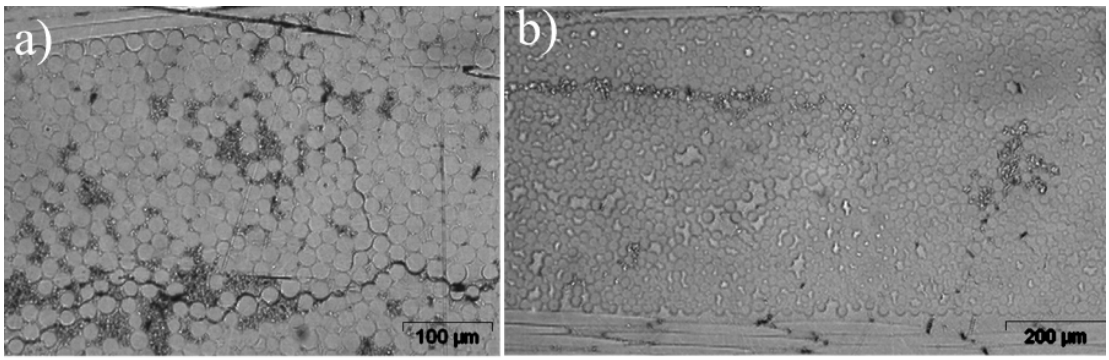

Fig. 5. Micrograph showing the occurrence of filler particles within bundles in laminates with: a) Susp B matrix, b) Susp C matrix

It now remains to scrutinize the results from the vacuum infusions. Assuming a stiff preform, Eq. (2) can be used to deduce the fiber preform permeability K from the experiments, see Fig. 6. To avoid influence from the flow at the edges, only the flow front positions in the middle of the preform was used to estimate the average flow front positions. The viscosity values used for the prediction of the permeability was obtained from the semi-empirical model given by Eq. (3). Other values used in the permeability estimation were $V_f = 0.5$, $\Delta p = 0.95$ bar.

From the results in Fig. 6 we see that a constant apparent permeability is obtained for the neat resin Susp A. For the particle suspensions B and C the apparent permeability initially increases with increasing flow lengths and appears to reach a constant value at 50 mm. The final permeability for Susp B and Susp C is however lower than the apparent permeability obtained with Susp A. Interestingly when measuring with Susp D the apparent permeability does not reach a constant value.

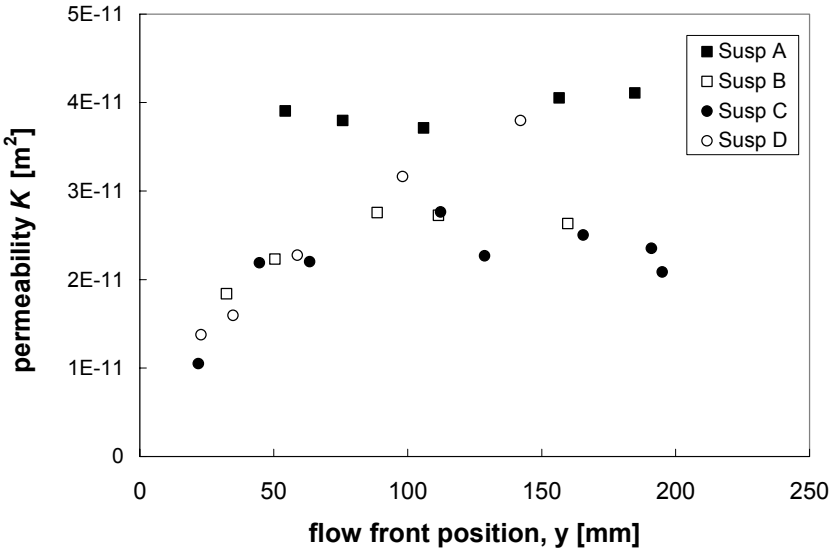

Fig. 6. Estimated permeability vs. flow front position from experiments.

The apparent initial increase in permeability for suspensions A and B is partially due to the fact that the pressure drop is measured over the whole system including the supplying pipes. Initially the losses in these pipes are in the same range as the losses in the fabric. Quite soon, however, the pressure drop in the pipes becomes negligible. The effect on the apparent permeability can be considered as negligible once the permeability has leveled off to a

constant value, cf. Fig. 6. Other factors likely to contribute to a fictitiously low initial permeability is the ill-defined region close to the distribution channel where volume fraction of fibers in average over entire material thickness is higher than in the preform and the inherent difficulties to determine $t = 0$ in the experiments. The lower constant apparent permeability found when using suspension B and C as compared to suspension A is likely to be caused by arrested particles seen in Fig. 3 and 4. Hindering the flow at certain positions will certainly decrease the apparent permeability. As to the flow properties stuck particles can be added to the solid phase implying a reduction in permeability, see for instance [13].

Interestingly the permeability does not decrease with flow length (and thereby with time) and our microscopy studies did not reveal any sign of systematic differences in particle concentration along the flow direction. This indicates that particle filtering over time has only minor influence on the overall macroscopic flow behavior. The densely packed and non-flowing regions seems thus to be formed relatively early during the infusion process soon after the first encounter of the preform with the flowing matrix. This scenario can supposedly be explained by the pore-doublet model by assuming that larger pressure gradients and/or higher flow rates on a local level decreases the risk for entrapment of the particles. The pressure over the two capillaries in this model will be the same but the flow rate through the smaller will naturally be lower, see Fig. 7. This may result in that the particles, by some mechanism, are stuck in the smaller capillary hindering the flow. By this blockage, the flow rate through, and the pressure gradient over the larger capillary will increase. An increase of flow through the larger capillary implies that the risk for complete blockage of flow in this capillary is reduced. Further accumulation of particles at this position is thus stopped.

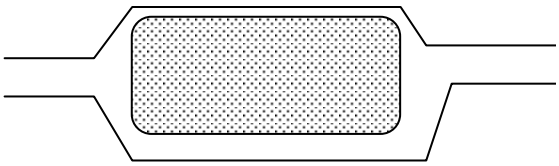

Fig. 7. Principal sketch of the pore-doublet model

A possible mechanism for the entrapment of the particles is that they are stuck where the local shear strain rate is low. For example will a simple analysis of flow through a circular tube yield the following expression for the maximum shear strain rate $\dot{\gamma}$ of the fluid

$$\dot{\gamma} = \frac{1}{2}\frac{\Delta p}{l\eta} r \tag{5}$$

where Δp denotes pressure difference between the ends of the tube (i.e. analogous to infusion pressure), l is the length of the tube and r is the radius of the tube. Maximum shear strain rate thus decreases with decreasing radius if other parameters remain constant. In analogy with the results for circular tubes it is therefore expected that the lowest strain rates during infusion should be attained in the regions where the irregularly shaped flow channel becomes narrow. Previous work reports that particles in a suspension under flow tends to migrate to regions where shear strain rates are low [14]. Flow can thus be stopped in these narrow sections if the strain rate becomes too low because of e.g. the Bingham type of behavior exhibited by the suspension. This plausible mechanisms can be amplified by the fact that the inter bundle channels often are filled before the bundles. Hence the bundles may act as filters leaving the

particles at the bundle wall and only letting the resin into the bundles. The particle concentration will, consequently, be higher at the bundle wall and so will σ_y. The observation of regions with extremely high particle concentrations at interfaces between bundles and flow channels reinforces this explanation.

Regarding the continuous increase in apparent permeability for Suspension D it is worthwhile mentioning that the data point at L = 150 mm is based on two observations only increasing the risk for misrepresentative results. Repeated experiments in the future are however obviously required (and planned) to facilitate the conclusion that the observed behavior for Susp D at long flow distances is not representative.

6. CONCLUSIONS

The work presented in this paper aims at identifying physically relevant mechanisms that govern the flow and subsequently the final particle distribution in fiber reinforced composites manufactured with infusion of a particle filled matrix suspension. It was found that the resin suspensions with ATH-particles exhibited a Bingham type of viscosity behavior. This feature can have a large influence on the mold filling process. If the strain rate in a section of a flow channel becomes too low e.g. because of unfavorable geometry of the flow channel, then no flow will occur in that section. Such a section can from a conceptual point of view be considered as if they were part of the porous structure providing resistance to flow and contributing to a reduction in apparent permeability rather than a flowing media. We believe that the presented work provides a good and physically sound foundation for future efforts that will aim at verifying the proposed mechanisms and eventually facilitate improved understanding and establishment of general guidelines for infusion with particle filled resin systems.

ACKNOWLEDGEMENTS

Funding for this work was provided by the SICOMP-foundation and the Faculty of Technology at Luleå University of Technology.

References

1. Sobolev, I, Woychesnin, E.A., “Alumina Trihydrate” In: Handbook of Fillers for Plastics, Katz H.S. (ed), Milewski J.V. (ed), Van Nostrand Reinhold, New York, USA, 1987
2. White S.R., Sottos N.R., Geubelle P.H., Moore J.S., Kessler M.R., Sriram S.R., Brown E.N., Viswanathan, S, “Autonomic healing of polymer composites”, *Nature*, 409 (2001), 794-797
3. Gebart B.R., Lundemo C.Y., Gudmundson P, “An evaluation of alternative injection strategies in RTM”, *Proc 47th Annual Conference of the Society of Plastics Institute*, Cincinnati, February 1992, USA
4. Gebart B.R., Gudmundson P, Strömbeck L.A., Lundemo C.Y., “Analysis of permeability in RTM reinforcements”, *Proc 8th International Conference on Composite Materials*, Honolulu, July 1991, USA.
5. Lundström T.S., “Void formation and transport in manufacturing of polymer composites”, Doctoral Thesis, Luleå University of Technology, Department of Mechanical Engineering, Division of Fluid Mechanics, 1996.
6. Holmberg J.A., “Resin transfer moulded composites: processing – structure – property relationships”, Doctoral thesis, Luleå University of Technology, Department of Materials and Manufacturing, Division of Polymer Engineering, 1997.
7. Barnes H.A., Hutton J.F., Walters K., “An introduction to Rheology”, Elsevier, Amsterdam, Netherlands, 1989
8. Patton T.C., “Paint flow and pigment dispersion”, Interscience, New York, 1964
9. Fernberg S.P., Öhgren I, “Rheology of ATH and unsaturated polyester suspensions – an evaluation of viscosity models”, SICOMP Technical Report, TR04-003, Piteå, Sweden, 2004
10. Gupta R.K., ”Particulate suspensions”, In: Volume 10, Composite Materials Series, Flow and rheology in polymer composites manufacturing, Advani S.G. (Ed), Elsevier Science B.V, Amsterdam, Netherlands, 1994.

11. Matijašić G., Glasnović A., ”Influence of dispersed phase characteristics on rheological behavior of suspensions”, *Chemical and Biochemical Engineering Quarterly*, 16 (2002), 165-172
12. Rossi S., Luckham P.F., Tadros Th.F., “Influence of non-ionic polymers on the rheological behavior of Na+-montmorillonite clay suspensions- I Nonylphenol-polypropylene oxide-polyethylene oxide copolymers”, *Colloids and Surfaces A: Physicochemical and Engineering Aspects*, 201 (2002), 85-100
13. Gebart, B.R., “Permeability of Unidirectional Reinforcements for RTM”, *Journal of Composite Materials*, 26 (1992), 1100-1133
14. Lam Y.C., Chen X., Tan K.W., Chai J.C., Yu S.C.M., “Numerical investigation of particle migration in poiseuille flow of composite system”, Composite Science and Technology, 64 (2004), 1001-1010